Journal of Neurochemistry, 2007, **103**, 736–748 doi:10.1111/j.1471-4159.2007.04809.x

Soluble oligomers from a non-disease related protein mimic Aβ-induced tau hyperphosphorylation and neurodegeneration

Marcelo N. N. Vieira,*,† Letícia Forny-Germano,*,‡ Leonardo M. Saraiva,* Adriano Sebollela,* Ana M. Blanco Martinez,§ Jean-Christophe Houzel,‡ Fernanda G. De Felice*,¶ and Sérgio T. Ferreira*

**Programa de Bioquímica e Biofísica Celular, Instituto de Bioquímica Médica, Universidade Federal do Rio de Janeiro, Rio de Janeiro, Brazil*
†Programa de Ciências Morfológicas, Universidade Federal do Rio de Janeiro, Rio de Janeiro, Brazil
‡Departamento de Anatomia, Universidade Federal do Rio de Janeiro, Rio de Janeiro, Brazil
§Departamento de Histologia e Embriologia, Instituto de Ciências Biomédicas, Universidade Federal do Rio de Janeiro, Rio de Janeiro, Brazil
¶Department of Neurobiology and Physiology, Northwestern University, Evanston, Illinois, USA

Abstract

Protein aggregation and amyloid accumulation in different tissues are associated with cellular dysfunction and toxicity in important human pathologies, including Alzheimer's disease and various forms of systemic amyloidosis. Soluble oligomers formed at the early stages of protein aggregation have been increasingly recognized as the main toxic species in amyloid diseases. To gain insight into the mechanisms of toxicity instigated by soluble protein oligomers, we have investigated the aggregation of hen egg white lysozyme (HEWL), a normally harmless protein. HEWL initially aggregates into β-sheet rich, roughly spherical oligomers which appear to convert with time into protofibrils and mature amyloid fibrils. HEWL oligomers are potently neurotoxic to rat cortical neurons in culture, while mature amyloid fibrils are little or non-toxic. Interestingly, when added to cortical neuronal cultures HEWL oligomers induce tau hyperphosphorylation at epitopes that are characteristically phosphorylated in neurons exposed to soluble oligomers of the amyloid-β peptide. Furthermore, injection of HEWL oligomers in the cerebral cortices of adult rats induces extensive neurodegeneration in different brain areas. These results show that soluble oligomers from a non-disease related protein can mimic specific neuronal pathologies thought to be induced by soluble amyloid-β peptide oligomers in Alzheimer's disease and support the notion that amyloid oligomers from different proteins may share common structural determinants that would explain their generic cytotoxicities.

Keywords: amyloid oligomers, cerebral cortex, hen egg white lysozyme, hippocampus, neurotoxicity, tau phosphorylation.

J. Neurochem. (2007) **103**, 736–748.

It has become clear in recent years that amyloid protein aggregates play crucial roles in important human pathologies, including Alzheimer's disease (AD), various forms of systemic amyloidosis and other disorders (Kelly 2000; Stefani and Dobson 2003; Ferreira *et al.* 2007). Despite the lack of sequence homology between distinct disease-related amyloid-forming proteins and peptides, the process of aggregation appears to be similar in all cases and the resulting materials share common tinctorial and morphological characteristics (Dobson 1999). In addition, recent studies have shown that the ability to form amyloid aggregates *in vitro* is not an exclusive property of proteins and peptides associated with disease but rather seems to be an intrinsic characteristic of polypeptide chains (e.g. Guijarro *et al.* 1998; Bouchard *et al.* 2000; Fandrich *et al.* 2001; Pertinhez *et al.* 2001; De Felice *et al.* 2004a).

Human lysozyme variants have been implicated in autosomal hereditary systemic amyloidosis (Pepys *et al.* 1993; Valleix *et al.* 2002; Yazaki *et al.* 2003). Single amino acid mutations in lysozyme have been shown to lead to structural destabilization of the variants and to an increased propensity to form amyloid aggregates (Booth *et al.* 1997). However, under partially denaturing *in vitro* conditions wild-type

Received April 24, 2007; accepted June 6, 2007.

Address correspondence and reprint requests to Fernanda G. De Felice or Sergio T. Ferreira, Instituto de Bioquímica Médica, Universidade Federal do Rio de Janeiro, Rio de Janeiro, RJ 21944-590, Brazil.
E-mails: felice@bioqmed.ufrj.br (FGF) or ferreira@bioqmed.ufrj.br (STF)

Abbreviations used: AD, Alzheimer's disease; Aβ, amyloid-beta peptide; Aβ42, amyloid beta peptide 1–42; DAPI, 4′,6-diamidino-2-phenylindole; EM, electron microscopy; HEWL, hen egg white lysozyme; MTT, 3-(4,5-dimethylthiazol-2-yl)-2,5-diphenyltetrazolium bromide; PBS, phosphate-buffered saline; SDS, sodium dodecyl sulfate; SEC, size-exclusion chromatography; TBS–T, Tris-buffered saline–Tween 20; ThS, thioflavin *S*; ThT, thioflavin T.

human lysozyme also forms amyloid aggregates similar to those formed by the variants (Morozova-Roche *et al.* 2000; De Felice *et al.* 2004a). Furthermore, hen egg white lysozyme (HEWL), a protein that is not associated with any disease, has recently been shown to undergo amyloid aggregation *in vitro* at acidic pH and high temperatures (Krebs *et al.* 2000). Those conditions destabilize the native structure of HEWL, favoring the population of aggregation-prone partially unfolded species. Lysozyme is easily obtained from different sources and its structure and folding mechanisms have been extensively characterized (Dobson *et al.* 1994). These features make lysozyme an interesting model for the study of amyloid aggregation.

Amyloid aggregates from various proteins that are associated or not with diseases have been shown to be toxic to different cell types (e.g. Bucciantini *et al.* 2002; Kayed *et al.* 2003; Sirangelo *et al.* 2004; Malisauskas *et al.* 2005). However, the precise mechanisms of toxicity have not been fully elucidated. In recent years, soluble protein oligomers have been increasingly recognized as emerging toxins in amyloid diseases (Ferreira *et al.* 2007; Haass and Selkoe, 2007). In particular, considerable evidence indicates that soluble amyloid beta peptide (Aβ) oligomers, rather than mature amyloid fibrils and plaques, are the main neurotoxins involved in the early pathogenesis of AD (for early studies, see Lambert *et al.* 1998; Wang *et al.* 2002; Walsh *et al.* 2002; reviewed in Klein 2006; Walsh and Selkoe 2004). For example, recent studies have shown that soluble Aβ oligomers induce tau hyperphosphorylation and neuronal oxidative stress, two major neuropathological hallmarks of AD (De Felice *et al.* 2007a,b). Tau plays important physiological roles in microtubule stabilization and dynamics, and its abnormal phosphorylation in AD is related to the formation of neurofibrillary tangles and to microtubule destabilization (Avila 2006).

In this study, we investigated the neuronal impact of soluble oligomers and amyloid fibrils from HEWL, a normally harmless, non-disease related protein. Under conditions promoting aggregation, HEWL initially forms β-sheet rich soluble oligomers, with the subsequent formation of amyloid fibrils. We found that HEWL oligomers-induced neuronal degeneration in cortical cultures and when injected into rat brains, whereas fibrils were virtually non-toxic. Interestingly, HEWL oligomers-induced tau hyperphosphorylation at AD-characteristic epitopes in cortical cultures, mimicking the effects of Aβ oligomers in neuronal cultures (De Felice *et al.* 2007b). These results indicate that neuronal pathologies that are characteristic of AD can be triggered by HEWL oligomers and support the notion that amyloid oligomers from different proteins may share common structural determinants that would explain their generic cytotoxicities (Bucciantini *et al.* 2002; Kayed *et al.* 2003). A deeper understanding of the toxic mechanisms triggered by soluble protein oligomers may allow the development of rational, effective treatments for different amyloid disorders.

Materials and methods

Chemicals

Hen egg white lysozyme, thioflavin T (ThT) and 3-(4, 5-dimethylthiazol-2-yl)-2, 5-diphenyltetrazolium bromide (MTT) were purchased from Sigma Chem. Co. (St Louis, MO, USA). Amyloid beta peptide 1–42 (Aβ42) was obtained from Bachem Inc. (Torrance, CA, USA). The Live/Dead assay kit was from Molecular Probes (Eugene, OR, USA). Mouse monoclonal anti-phosphotau (phosphoepitopes Ser202/Thr205) antibody (AT-8 antibody) was obtained from Innogenetics SA (Gent, Belgium). Rabbit polyclonal anti-phosphotau (Ser404) antibody (P404 antibody) was from Santa Cruz Biotechnology (Santa Cruz, CA, USA). Murine monoclonal anti-total tau (Tau-C) antibody was from Dako (Glostrup, Denmark). The A11 rabbit polyclonal anti-oligomer antibody was from Chemicon (Temecula, CA, USA). Fluoro-Jade C was obtained from HistoChem Inc. (Jefferson, AR, USA).

HEWL aggregation

One mmol/L solutions of HEWL (Sigma Chem. Co.) were prepared in unbuffered H_2O at pH 2.0 (pH adjusted to 1.85 with HCl before the addition of protein, resulting in a final pH 2 solution). Aliquots were incubated at 65°C for different times and were utilized as described below. Incubation of HEWL at 65°C was planned so that samples corresponding to different aggregation states would be simultaneously ready for use in cell culture or *in vivo* experiments. Control HEWL samples maintained for up to 1 week at 4°C showed no sign of aggregation or toxicity by any of the criteria described below.

Turbidity, thioflavin T fluorescence and circular dichroism measurements

Aggregation was monitored at 23°C by ThT fluorescence measurements (λ_{exc} = 440 nm; λ_{em} = 485 nm) on a Molecular Devices Gemini-XS fluorescence plate reader (Molecular Devices, Sunnyvale, CA, USA) and by turbidity measurements at 340 nm on 10-fold diluted aliquots. Circular dichroism measurements were carried out at 23°C on 50-fold diluted aggregated HEWL aliquots on a Jasco J-715 spectropolarimeter (Jasco Inc., Easton, MD, USA) using a 0.1-cm pathlength cuvette. Secondary structure contents were calculated using three different algorithms included in the CDPro package (http://lamar.colostate.edu/~sreeram/CDPro) (Sreerama and Woody 2000).

Size-exclusion chromatography and non-denaturing gel electrophoresis

Size-exclusion chromatography (SEC) was carried out on a Superdex-200 column (Amersham Biosciences, Uppsala, Sweden) equilibrated in water/HCl, pH 2.0, containing 250 mmol/L NaCl, and connected to a Shimadzu LC-10AD HPLC system (Shimadzu Scientific Instruments, Columbia, MD, USA). Aliquots (300 μg protein) of HEWL were applied onto the column and elution was monitored by absorption at 280 nm. Non-denaturing agarose

electrophoresis was carried out in 25 × 18 cm horizontal 0.8% agarose gels. The running buffer used was 50 mmol/L Tris–HCl, pH 7.5, containing 384 mmol/L glycine. As expected due to its high-isoelectric point, lysozyme migrates to the negative pole. Protein bands were visualized by Coomassie Brilliant Blue staining.

Immunoblot analysis of HEWL oligomers

Dot immunoblot analysis was carried out to investigate the reactivity of the anti-oligomer A11 antibody (Chemicon) against HEWL soluble oligomers. To this end, 1.4 and 14 μg aliquots from HEWL samples aggregated for 0, 24, or 96 h were spotted onto nitrocellulose membranes and air dried for 60 min. Membranes were blocked for 2 h with 5% non-fat milk in Tris-buffered saline–Tween 20 (TBS–T; 10 mmol/L Tris, pH 7.2, 150 mmol/L NaCl, and 0.1% Tween 20) and incubated with A11 antibody (1 : 2000 dilution) for 4 h at 23°C. Following three 10 min washes with TBS–T, the membranes were probed with horseradish peroxidase-conjugated anti-rabbit IgG secondary antibody and dots were visualized with the ECL Plus chemiluminescence assay (Amersham Biosciences).

Neuronal cultures and neurotoxicity assays

Timed pregnant female Sprague–Dawley rats were used. Cerebral cortices from 15-day-old embryos were dissected and cultured as previously described (De Felice *et al.* 2004b). Briefly, the brains were removed and placed in a petri dish containing phosphate-buffered saline (PBS) -glucose solution. The cortices were dissected and, after stripping away the meninges, neurons were gently mechanically dissociated in PBS-glucose, centrifuged at 4°C for 4 min at 1000 *g*, and resuspended in Neurobasal medium supplemented with B27. Dissociated cells were plated on poly lysine-treated plates at a density of 1000–1500 cells/mm^2 and were incubated at 37°C in a humidified atmosphere of 5% CO_2.

Hen egg white lysozyme monomers, oligomers, or fibrils (prepared at pH 2, as described above, and derived from a single HEWL stock solution) were added to the cultures after 5 days *in vitro* and were kept in the medium for 48 h. Aliquots from the 1 mmol/L HEWL preparations were 50- or 200-fold diluted in culture medium (resulting in final concentrations of 20 or 5 μmol/L HEWL, respectively, as described in Results). Control measurements showed that addition of HEWL preparations at pH 2 or of the corresponding low amounts of vehicle (H_2O/HCl at pH 2) alone caused no changes in the pH of the buffered culture medium (data not shown). For investigation of Aβ42 toxicity, the lyophilized Aβ42 was dissolved in a 50% solution of trifluoroethanol in water, and aliquots were directly added from this 2 mmol/L stock solution to the culture medium (100-fold dilution, resulting in a final Aβ42 concentration of 20 μmol/L).

Cell viabilities were assessed using the Live/Dead assay (Molecular Probes) following manufacturer's instructions. Randomly chosen fields were examined and counted in a Nikon Eclipse TE300 microscope (Nikon, Kanagawa, Japan). Five different fields (~200 cells per field) were examined per well and two cultures were used per experimental condition. For the MTT assay, cultures were incubated for 4 h in the presence of 0.5 mg/mL MTT. One hundred microliters of cell lysis buffer [10% sodium dodecyl sulfate (SDS) and 0.01 mol/L HCl] were then added to each well and the samples were incubated overnight at 37°C in a humidified incubator. Absorption was measured at 540 nm in a plate reader. Three independent experiments (each with duplicate wells per experimental condition) were carried out with different neuronal cultures. Cell culture solutions were prepared and kept at all times under sterile conditions. For both Live/Dead and MTT assays, statistical significances of differences between vehicle-treated cultures and other experimental conditions were evaluated by *t*-test analysis (one-tailed) and corresponding *p*-values are indicated in the legend to Fig. 3.

Immunofluorescence and immunoblotting

For immunocytochemistry, primary cultures of cortical neurons were exposed to HEWL monomers, oligomers, or fibrils for 24 h and were fixed for 20 min with 4% *p*-formaldehyde in 0.01 mol/L PBS followed by blocking and permeabilization in PBS containing 2.5% bovine serum albumin and 0.3% Triton X-100. After 30 min, the cells were incubated for 4 h with mouse anti-phosphotau (phosphoepitopes Ser202/Thr205) primary antibody (AT-8 antibody). After washing, the cells were incubated for 2 h with anti-mouse IgG conjugated to FITC. The cells were again washed and mounted for fluorescence microscopy.

For immunoblotting, cortical neurons exposed to HEWL for 6 h were rinsed with PBS supplemented with 1 mmol/L phenylmethylsulfonyl fluoride, and then lysed in 50 mmol/L Tris–HCl, pH 7.5, 1% SDS, 150 mmol/L NaCl, 1 mmol/L EDTA, 20 mmol/L sodium pyrophosphate, 20 mmol/L sodium fluoride, 1 mmol/L sodium *o*-vanadate, 1 mmol/L phenylmethylsulfonyl fluoride, 1 μmol/L okadaic acid, and a cocktail of protease inhibitors (10 μg/mL of aprotinin, leupeptin, and pepstatin). Samples (20 μg protein per lane) were resolved in 10% SDS–polyacrylamide gel electrophoresis gels followed by transfer to nitrocellulose membranes. Membranes were blocked for 2 h with 5% non-fat milk in TBS–T followed by overnight incubation with rabbit polyclonal anti-phosphotau (Ser404) antibody (P404 antibody) at 4°C. Immunoreactive bands were visualized using peroxidase-conjugated secondary antibody (Amersham Biosciences; 1 : 4000 dilution; 2 h at 23°C) and chemiluminescence detection (ECL Plus; Amersham Biosciences). Loading controls were performed by probing the same nitrocellulose membrane with murine monoclonal anti-total tau (Tau-C; 1 : 2000 dilution) and with anti-cyclophilin B (1 : 4000 dilution; Affinity Bioreagents, Golden, CO, USA) antibodies. Densitometric scanning and quantitative evaluation of the intensities of protein bands were carried out using Image J software (NIH, Bethesda, MD, USA; Windows version) (Abramoff *et al.* 2004). Immunoblots were carried out using six different neuronal cultures (prepared from embryos obtained from three pregnant rats) treated with three different HEWL preparations, and results in different experimental conditions are presented as the ratio between P404 tau immunoreactive and total tau band intensities. Statistical significances of differences between vehicle-treated samples and other experimental conditions were evaluated by *t*-test analysis (one-tailed) and corresponding *p*-values are indicated in Fig. 3b.

Electron microscopy

Transmission electron microscopy (EM) images were acquired on a Jeol 1200-EX microscope (Nikon, Tokyo, Japan) operating at 80 kV. Five microliters of samples were placed on Formvar/carbon-coated nickel grids and blotted off after 2 min. Samples were stained with 5 μL of 1% uranyl acetate, air-dried, and observed at

magnifications of 20 000–50 000×. Images were analyzed using NIH Image J (Abramoff *et al.* 2004) in order to obtain size distributions for the HEWL oligomers.

In vivo intracerebral HEWL injections

Male adult Wistar rats (280–320 g) were given 0.2 mg/kg atropine and anesthetized with 50 mg/kg ketamine and 40 mg/kg xylazine (i.m.) and were placed in a stereotaxic frame. A small craniotomy was performed over the parietal cortex (Area S1, standard coordinates: A 7.0 mm; L 5.0 mm; H 8.0 mm) and 1.5 μL of vehicle (H_2O/HCl at pH 2) or HEWL samples (1.5 nmol total protein, expressed as HEWL monomers) in different states of aggregation (see Results) were injected through a glass micropipette connected to a Hamilton syringe. In order to allow direct comparison between the effects of HEWL oligomers versus monomers or fibrils, oligomers were always injected in one cerebral hemisphere, while the other hemisphere of the same animal received injections of vehicle, monomers, or fibrils, in a total of 15 animals. As an additional control, one animal was sham-operated in one hemisphere, i.e. underwent all surgical procedures including introduction of the micropipette but received no injections.

The animals were killed 8 days later. After transcardiac perfusion with saline followed by 4% *p*-formaldehyde, some brains were embedded in paraffin and microtome-cut in 8-μm thick sections used for cresyl violet and hematoxylin-eosin staining to verify the overall cytoarchitecture. For thioflavin *S* (ThS) -staining of fibrillar amyloid aggregates, Fluoro-Jade C (HistoChem Inc.) staining of degenerating neurons (as described in Schmued *et al.* 2005) or 4′,6-diamidino-2-phenylindole (DAPI) counter-staining of cell nuclei, brains were cryoprotected in 30% sucrose and frozen-cut into 30-μm thick coronal sections. Images from all sections were acquired on a Zeiss Axioplan microscope (Zeiss, Jena, Germany). Relevant regions, with standard stereotaxic coordinates given in mm, were selected as follows: cerebral cortex immediately below the injection site (A 7.0, L 5.0, H 7.0), cortex connected to the injected region (area S2, A 7.0, L 6.5, H 5.0), thalamus (A 5.0, L 3.2, H 4.0), hippocampus (A 5.0, L 3.7, H 6.0), and amygdala (A 7.0, L 5.2, H 0.5). Low- and high-power photomicrographs were systematically taken from those regions using a Zeiss HR Axiocam camera and were compared across conditions.

Results

Kinetics of HEWL amyloid aggregation

Hen egg white lysozyme aggregation was induced by incubation at pH 2.0 and 65°C. Under these conditions, the native state of HEWL is destabilized but intermolecular interactions are still favored, and previous studies have shown that HEWL adopts a partially unfolded structure that aggregates into amyloid fibrils upon prolonged incubation (Krebs *et al.* 2000). In order to characterize in more detail the kinetics of HEWL aggregation, samples incubated for periods ranging from a few hours to several days were examined by a number of biochemical and biophysical techniques. Aggregation was characterized by an initial lag phase (lasting ~2 days), followed by sharp increases in both turbidity (optical density at 340 nm) and ThT fluorescence (Fig. 1a). It is interesting to note that no changes in ThT fluorescence were detected for up to 48 h of incubation, whereas a discrete but reproducible increase in turbidity was detectable within this period (Fig. 1a). This suggested that the HEWL aggregates formed at the early stages of aggregation did not possess a characteristic amyloid structure that would give rise to ThT binding. Circular dichroism measurements in the same samples revealed a significant increase in β-sheet content and a parallel decrease in α-helix content during the first 48 h of incubation (Fig. 1b).

The initial stages of HEWL aggregation were further investigated by SEC analysis. Control HEWL samples (not incubated at high temperature) eluted from the column as a single peak corresponding to lysozyme monomers (Fig. 1c). After 12 h of incubation at 65°C, HEWL monomers partially converted to higher molecular weight species exhibiting shorter retention times in the column. At 24 h, the peak corresponding to the monomer completely disappeared and a single, broad peak was detected, likely corresponding to a heterogeneous population of higher molecular weight species (Fig. 1c). It is noteworthy that native monomeric HEWL eluted from the column at a retention volume larger than expected for a protein of the molecular mass of lysozyme, likely reflecting interactions of the protein with the gel matrix under our experimental conditions. This precluded a detailed analysis of the molecular masses of the species formed upon aggregation. However, the data clearly indicated the conversion of monomeric HEWL into higher molecular mass species within the first 24 h of aggregation. No indication of the presence of very large aggregates (eluting at the exclusion volume of the column) was observed in the analysis of samples aggregated for up to 24 h, consistent with the notion that fibrils were not present in such samples (Fig. 1c, inset). SEC analysis of samples incubated for periods longer than 24 h were not carried out because of the expected presence of large, insoluble amyloid fibrils in such samples (see below).

Non-denaturing agarose gel electrophoresis also revealed a progressive aggregation of HEWL as a function of incubation time (Fig. 1d). Within the first 24 h, HEWL monomers progressively converted into a polydisperse, heterogeneous population of higher molecular mass species, as indicated by the smears in the corresponding gel lanes. Analysis of the smears indicated that the aggregates formed after 6 h were more heterogeneous in size than the aggregates formed at 24 h. After 48 h (and in longer incubation times), those species were progressively converted into even larger sized particles that did not penetrate the agarose gel (Fig. 1d).

Control measurements showed that samples kept under otherwise identical solution conditions but at 4°C (indicated as the 'zero time' of incubation at 65°C in Fig. 1) remained monomeric and exhibited native-like secondary structures for the duration of the experiments (5 days), confirming that

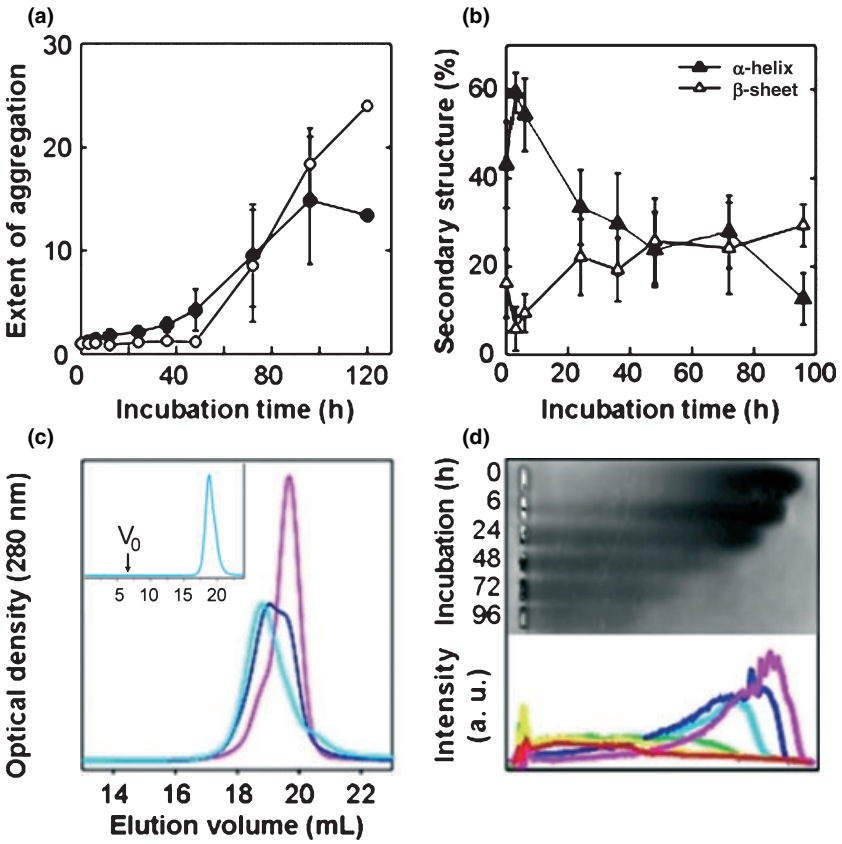

Fig. 1 Kinetic and conformational analysis of hen egg white lysozyme (HEWL) aggregation. HEWL (1 mmol/L) was incubated in water/HCl, pH 2.0, at 65°C for different time intervals ranging from 6 h to 5 days. At different times, aliquots were withdrawn and the aggregation state and conformation of HEWL were monitored using different techniques. Panel (a): Optical density at 340 nm (closed circles) and thioflavin T fluorescence emission (open circles) measurements as a function of aggregation time. Symbols correspond to mean ± SD from three independent determinations. Panel (b): Far-UV circular dichroism analysis; secondary structure contents were determined as described in Materials and methods. Symbols correspond to mean ± SD from three independent determinations. Panel (c): Size-exclusion chromatography analysis of monomeric HEWL (purple) or samples aggregated for 12 h (dark blue) or 24 h (cyan). The *inset* shows the complete chromatographic run of the HEWL sample incubated for 24 h and shows that no large aggregates are detectable at lower elution volumes. The void volume (V_0) of the column is indicated by the vertical arrow. Panel (d): Native agarose gel electrophoresis (top) and corresponding densitometric analysis (bottom) of samples aggregated for increasing time periods (from purple to red in bottom panel).

amyloid aggregation was induced by partial unfolding of HEWL caused by combined high temperature and low pH. The kinetics of HEWL aggregation under the conditions described above were highly reproducible, as revealed by routine characterization of different preparations by turbidimetry, ThT binding, circular dichroism, and SEC analysis. This allowed us to obtain relatively pure preparations of HEWL monomers, oligomers, or fibrils, by incubating the protein at high temperature for different periods of time and to analyze the morphology and biological activity of each conformation separately.

Morphologies of HEWL aggregates

Transmission EM analysis of HEWL samples aggregated for 6 h revealed the presence of roughly spherical aggregates heterogeneous in size, ranging from 14 to 47 nm in diameter (average diameter 32 ± 8 nm; Fig. 2a). Samples examined after 24 h of incubation exhibited a heterogeneous population of smaller oligomers (average diameter 18 ± 4 nm) (Fig. 2b). These observations suggest that the larger spherical aggregates that are more prominent at the early stages of aggregation (6 h) shrink into more compact aggregates with increasing incubation times. A recent investigation of the aggregation of transthyretin showed a similar shrinkage of the sizes of spherical aggregates with increasing aggregation times (Lindgren *et al.* 2005). These observations suggest the possibility that there are different pathways for the formation of the smaller and larger aggregates, with the latter species being kinetically favored and the former corresponding to a more stable, thermodynamically favored state. We also note that the size distribution of the spherical amyloid aggregates

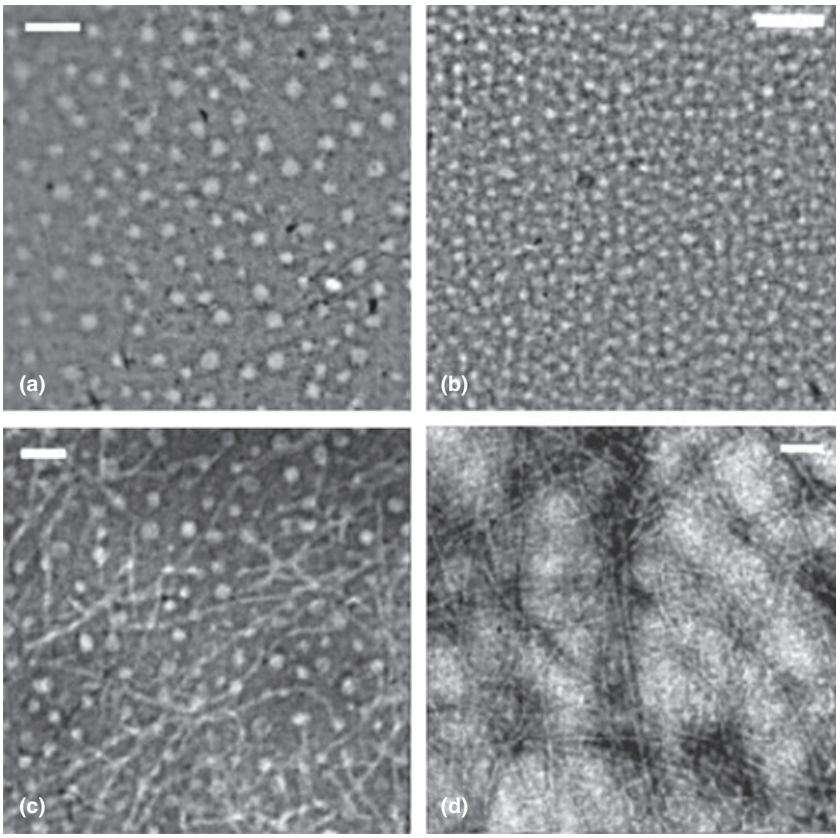

Fig. 2 Transmission electron microscopy analysis of hen egg white lysozyme aggregates. Representative electron micrographs showing abundant roughly spherical hen egg white lysozyme oligomers formed after 6 h (panel a) or 24 h of aggregation (panel b), a mixture of oligomers and immature amyloid fibrils present after 48 h of aggregation (panel c), and mature amyloid fibrils formed after 5 days of aggregation (panel d). Scale bars: 150 nm.

formed by HEWL are within the range of values reported for aggregates formed by various other proteins (e.g. Hoshi *et al.* 2003; Lashuel *et al.* 2003; Nandi and Nicole 2004; Ray *et al.* 2004; Lindgren *et al.* 2005).

Formation of HEWL spherical aggregates took place well before any significant increase in ThT fluorescence (Fig. 1a) and concomitantly with the conformational transition from the predominantly α-helical lysozyme monomers to a β-sheet rich conformational state (Fig. 1b). After 48 h of aggregation, a mixture of oligomers and immature amyloid fibrils were observed by EM (Fig. 2c). By the fifth day of aggregation, HEWL oligomers had completely disappeared and only well-defined, mature amyloid fibrils could be observed (Fig. 2d). Together with the SEC and agarose gel electrophoresis results described above, these results suggest that HEWL aggregation is a process in which monomers initially give rise to a heterogeneous population of oligomers which convert into large amyloid fibrils upon prolonged incubation.

Immunoanalysis of HEWL oligomers

A11, an antibody raised against a synthetic mimic of Aβ oligomers, has been shown to cross-react with soluble oligomers from other amyloidogenic proteins, but not with the corresponding natively folded proteins or with amyloid fibrils (Kayed *et al.* 2003). This suggests that a shared conformation of the oligomers is recognized by the antibody (Kayed *et al.* 2003), which led us to investigate whether A11 would also recognize HEWL oligomers prepared following our protocol. However, the A11 antibody (commercially available from Chemicon) did not react with HEWL oligomers in dot blot assays (data not shown).

HEWL oligomers are neurotoxic to cortical neurons in culture

Obtaining relatively pure, well-characterized preparations of HEWL in different states of aggregation allowed us to investigate the toxicities of the different types of aggregates. We used primary cortical neurons as a model because amyloid oligomers from different proteins appear to be causatively related to several neurodegenerative disorders (Klein 2006; Ferreira *et al.* 2007; Haass and Selkoe 2007). Cortical neurons were exposed for 48 h to HEWL monomers, oligomers (obtained after 24 h of aggregation), and fibrils (obtained after >96 h of aggregation), and neurotoxicity was determined using both Live/Dead (cell viability) and MTT reduction assays (Fig. 3). As expected, neurons treated with HEWL monomers exhibited similar viabilities as control (vehicle-treated) cultures (Fig. 3a, c, and d). Interestingly, cultures treated with 5 μmol/L HEWL oligomers exhibited a marked decrease in neuronal viability (Fig. 3a and e), whereas

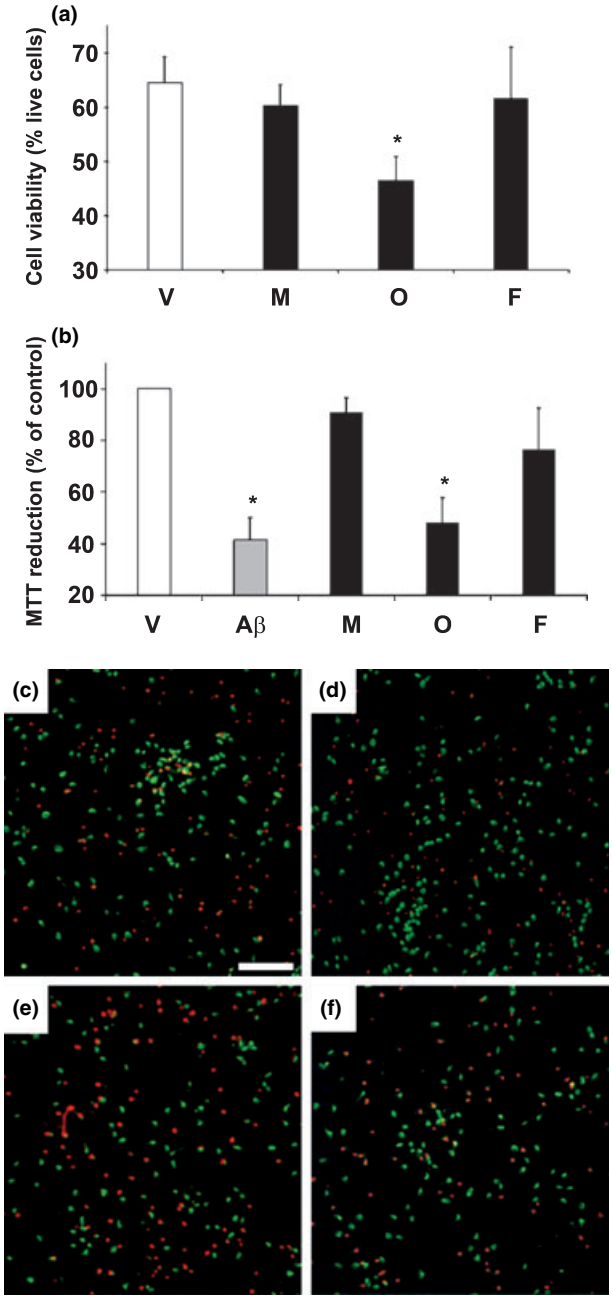

Fig. 3 Neuronal damage induced by hen egg white lysozyme (HEWL) aggregates. Panel a: Neuronal viability measured with the Live/Dead assay after exposure of cortical neuronal cultures for 48 h to either vehicle or 5 μmol/L HEWL monomers (M), oligomers (O), or fibrils (F). HEWL oligomers and fibrils were obtained after 24 or 72 h of aggregation, respectively. Bars represent mean ± SD results for three cultures. Panel b: MTT [3-(4, 5-dimethylthiazol-2-yl)-2, 5-diphenyltetrazolium bromide] reduction assay of cortical neuronal cultures after exposure for 48 h to either vehicle or 20 μmol/L HEWL monomers (M), oligomers (O), or fibrils (F). HEWL oligomers and fibrils were obtained after 24 or 72 h of aggregation, respectively. The toxicity of 20 μmol/L amyloid beta peptide 1–42 (Aβ42) under identical experimental conditions is shown for comparison. Bars represent mean ± SD for three independent experiments in duplicate. HEWL oligomers exhibited statistically significant toxicities (*$p < 0.005$) compared with control (vehicle-treated) cultures in both Live-Dead and MTT assays, whereas fibrils showed virtually no toxicity. Panels (c–f): Representative Live/Dead images (live cells shown by green calcein fluorescence and dead cells by red ethidium homodimer fluorescence) of cortical neuronal cultures exposed to vehicle (c), monomeric (d), oligomeric (e), or fibrillar (f) HEWL. Scale bar corresponds to 100 μm.

5 μmol/L HEWL fibrils were not toxic in those experiments (Fig. 3a and f). Neuronal damage induced by HEWL oligomers was further investigated using the MTT reduction assay. The results obtained using MTT were quite similar to those obtained with the Live/Dead assay: HEWL oligomers, but not monomers or fibrils, significantly impaired MTT reduction (Fig. 3b). It is also noteworthy that in MTT experiments the extent of neuronal damage induced by 20 μmol/L HEWL oligomers was comparable with that induced by the same concentration of Aβ42 (Fig. 3b), which is known to be highly toxic to neurons in culture.

HEWL oligomers induce tau hyperphosphorylation in cortical neurons in culture

Because HEWL oligomers induced neurotoxicity in cortical cultures to an extent that was comparable with that caused by Aβ (Fig. 3), we next sought to determine whether HEWL aggregates might also instigate neuronal tau hyperphosphorylation, a major facet of AD that is known to be induced by Aβ oligomers (De Felice *et al.* 2007b). Primary cultures of cortical neurons were treated for 6 h with vehicle or with 20 μmol/L HEWL monomers, oligomers, or fibrils, and phosphotau levels were analyzed by immunocytochemistry and by western blotting at a number of phosphoepitopes (Ser202/Thr205, Thr212/Ser214, and Ser404) that are characteristically phosphorylated in AD (Zheng-Fischhofer *et al.* 1998; Hampel *et al.* 2003; Maccioni *et al.* 2006).

Immunocytochemistry using the AT-8 antibody (Ser202/Thr205 phosphoepitopes) showed that 20 μmol/L HEWL oligomers, as well as 20 μmol/L HEWL fibrils, promoted abnormal tau phosphorylation in cortical neurons compared with cultures treated with either vehicle or HEWL monomers (Fig. 4a). Tau hyperphosphorylation was significant at 6 h of treatment with HEWL oligomers and remained elevated for 24 h, similar to what has been recently reported for tau phosphorylation induced by Aβ oligomers (De Felice *et al.* 2007b). Similar results were obtained using the AT100 antibody (tau phosphoepitopes Thr212/Ser214; data not shown). In accord with these results, western blot analysis with the P404 antibody showed that the P-Ser404/total tau ratio was significantly increased in cultures treated with HEWL oligomers and fibrils compared with vehicle- and monomer-treated cultures (Fig. 4b). Additional loading con-

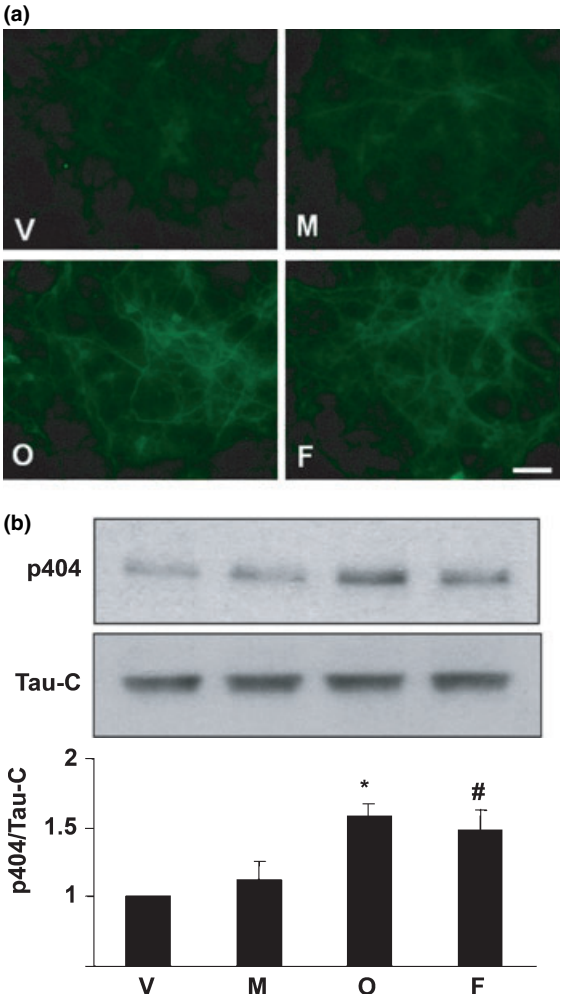

Fig. 4 Abnormal tau phosphorylation induced by hen egg white lysozyme (HEWL) aggregates in cortical neuronal cultures. Panel (a): Immunofluorescence using AT-8 antibody. Images (representative from two different experiments) are shown for cultures treated for 24 h with vehicle, or with HEWL monomers, oligomers, or fibrils, as indicated. The scale bar corresponds to 50 μm. Panel (b): Immunoblots using P404 antibody of cortical neuronal cultures treated for 6 h with vehicle (V), monomeric (M), oligomeric (O), or fibrillar (F) HEWL. Control measurements showed that total tau levels (measured using the Tau-C antibody and anti-cyclophilin B as a loading control) were not affected by the presence of HEWL aggregates. Panel (b) also shows quantitative analysis of P-Ser404 levels normalized by total tau (Tau-C immunoreactivity) in cultures treated with different HEWL aggregates. Normalization of P-Ser404 immunoreactivity by cyclophilin B as an additional loading control yielded similar results (not shown). The bars represent mean ± SD from experiments with six different cultures treated with three different HEWL preparations. Statistically significant differences with respect to vehicle-treated cultures are indicated by the symbols *($p < 0.004$) and #($p < 0.015$).

trols using anti-cyclophilin B antibody yielded similar results and showed that total tau levels (detected by the tau-C antibody) were unaffected by HEWL treatment (not shown).

It is interesting to note that while both HEWL oligomers and fibrils instigated tau hyperphosphorylation (Fig. 4), under our experimental conditions HEWL fibrils were little or non-toxic to cortical neurons in culture (Fig. 3). This observation is consistent with tau phosphorylation representing an early stage in neurodegeneration, as recently suggested for tau phosphorylation induced by Aβ oligomers (De Felice *et al.* 2007b). It also suggests the possibility that HEWL oligomers, but not fibrils, activate other neuronal signaling pathways that lead to neurodegeneration within the time window investigated in our studies.

In vivo neurodegeneration induced by HEWL oligomers

In order to investigate the neuronal impact of HEWL aggregates *in vivo*, monomers, oligomers, or fibrils were stereotaxically injected into the parietal cortex of adult rats. To allow direct comparison between the effects of different types of aggregates, 1.5 nmol HEWL oligomers were injected into one cerebral hemisphere of each animal, while the other hemisphere of the same animal received injections of either vehicle or 1.5 nmol of HEWL monomers or fibrils. After 7 days, the animals were killed and the brains were processed for histological analysis. Figure 5b shows representative ThS-stained coronal sections from an animal injected with HEWL fibrils in the right hemisphere and with HEWL oligomers in the left hemisphere. In seven different animals examined, presence of ThS-positive amyloid deposits was observed in hemispheres injected with fibrils, but not in hemispheres injected with oligomers (Fig. 5b) or monomers (not shown). This indicates that injected HEWL monomers and oligomers remained soluble and did not form detectable fibrillar deposits in the brain milieu for the duration of our experiments (7 days).

In initial experiments, coronal sections from the brains of animals injected with HEWL oligomers in the left hemisphere and monomers in the right hemisphere were stained with cresyl violet and hematoxylin-eosin for inspection of the overall cytoarchitecture. Those experiments suggested that injection of oligomers, but not monomers, caused neurodegeneration and disorganization of the cytoarchitecture in some brain regions (e.g. in the hippocampus; data not shown). These results prompted us to evaluate in more detail the impact of HEWL aggregates *in vivo.* To this end, Fluoro-Jade C staining of degenerating neurons (Schmued *et al.* 2005) was performed in sections from hemispheres injected with vehicle, oligomers, or fibrils. Inspection of the staining patterns across the entire oligomer-treated hemispheres revealed that some areas exhibited prominent Fluoro-Jade staining. Those regions were selected for detailed analysis and included the cerebral cortex immediately below the injection site (area S1), the neighboring cortical region S2, thalamus, hippocampus, and amygdala (Fig. 5a). Figure 5c shows low- and high-magnification images of DAPI and Fluoro-Jade C staining of the hippocampus in a hemisphere

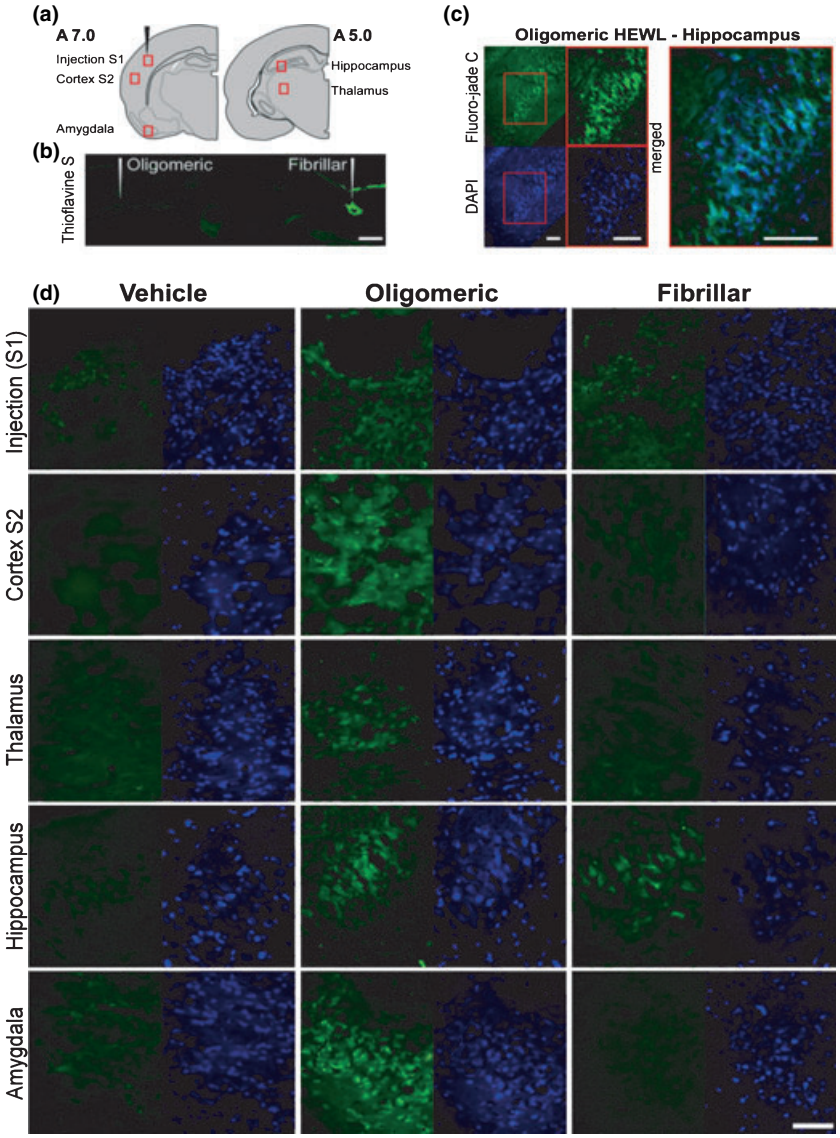

Fig. 5 *In vivo* neurodegeneration induced by hen egg white lysozyme (HEWL) oligomers. Coronal sections of rat brains were obtained 8 days after injection of 1.5 μL of vehicle or 1.5 nmol (in 1.5 μL) of HEWL oligomers or fibrils into the parietal cortex (area S1). Panel (a): Schematic representation of coronal sections at AP levels 7.0 and 5.0, showing the location of the injection site (indicated by a black pipette) and of the five selected regions of interest (red boxes) shown in panel (d). Panel (b): Representative images of thioflavin *S*-stained coronal sections showing the presence of insoluble amyloid deposits at the site of injection of fibrils (right) and absence of deposits in the other hemisphere of the same animal, which was injected with oligomers (left). Panel (c): Representative photomicrographs of the hippocampus CA3 field of one hemisphere injected with oligomers. Left: low- and high-power magnification views of the hippocampal region of interest stained for degenerating neurons with Fluoro-Jade C (green) and for cell nuclei with 4′,6-diamidino-2-phenylindole (DAPI; blue). Right: merged images of Fluoro-Jade C and DAPI staining. Panel (d): Representative photomicrographs (40× objective) of Fluoro-Jade C and DAPI staining of the five selected regions indicated in (a), taken from six different hemispheres injected with vehicle (left column), HEWL oligomers (middle column), or fibrils (right column). From top to bottom: cerebral cortex immediately below the injection site (area S1), cortex connected to the injected region (area S2), thalamus, hippocampus, and amygdala. Scale bars: 500 μm in (b) and 50 μm in (c and d).

injected with oligomers. Figure 5d shows representative images of Fluoro-Jade C and corresponding DAPI stainings from the five selected regions from six different hemispheres injected with vehicle, oligomers, or fibrils. Control non-operated and sham-operated animals showed no Fluoro-Jade staining in any of the brain regions analyzed (data not shown). With the exception of the area immediately surrounding the injection site, little or no Fluoro-Jade C staining was detected in hemispheres injected with vehicle (Fig. 5d, left column). In contrast, consistent staining was

observed in the five selected regions in hemispheres injected with HEWL oligomers (Fig. 5d, middle column). Among the five selected regions, the most prominent and consistent labeling was detected in the amygdala. Consistent with cresyl and hematoxylin-eosin staining, neuronal degeneration induced by HEWL oligomers was also revealed by Fluoro-Jade staining in the hippocampus. Injection of HEWL fibrils produced neurodegeneration at the injection site and less intense labeling in some of the observed fields in the hippocampus and S2 cortex (Fig. 5d, right column).

Discussion

Recent studies have shown that, in addition to disease-related amyloid-forming proteins and peptides, proteins that are not normally associated with disease can also form amyloid aggregates (oligomers, protofibrils, and fibrils) under conditions that destabilize their native structures (e.g. Guijarro *et al.* 1998; Bouchard *et al.* 2000; Fandrich *et al.* 2001; Pertinhez *et al.* 2001; De Felice *et al.* 2004a). The underlying notion is that destabilization of protein structure leads to population of partially folded species that are prone to aggregation (Ferreira *et al.* 2006). Reduced thermodynamic stability may explain the general observation that disease-related proteins assemble more readily than non-disease related proteins. In the specific case of human lysozyme, for example, genetic variants that are associated with hereditary amyloidosis have been shown to exhibit reduced thermodynamic stabilities compared with wild-type lysozyme (Booth *et al.* 1997; Morozova-Roche *et al.* 2000; Canet *et al.* 2002).

In some cases, amyloid aggregates have been shown to be cytotoxic to different cell types (e.g. Bucciantini *et al.* 2002; Sirangelo *et al.* 2004; Malisauskas *et al.* 2005). In recent years, soluble protein oligomers have been increasingly recognized as emerging toxins in AD and other amyloidoses (Klein *et al.* 2004; Selkoe and Haass, 2007; Ferreira *et al.* 2007). Indeed, for an increasing number of diseases, levels of soluble oligomers of the corresponding proteins/peptides appear to be closely associated with pathology, while the correlation between amyloid fibril burden and pathology is not necessarily evident (reviewed in Ferreira *et al.* 2007).

In the present work, we showed that HEWL, a normally harmless, non-disease related protein, forms different types of amyloid aggregates under conditions that destabilize its native conformation. Partial unfolding of HEWL was achieved by incubation at acidic pH at the transition mid-point for thermal unfolding (Tm) for heat denaturation of the protein (Krebs *et al.* 2000). Previous studies have shown that incubation under partially denaturing conditions also leads to formation of various types of aggregates from human lysozyme variants associated with systemic amyloidosis (Morozova-Roche *et al.* 2000; De Felice *et al.* 2004a; Vieira *et al.*, 2006). Soluble HEWL oligomers, formed at the early stages of aggregation, were toxic to cortical neurons in culture and instigated pronounced neurodegeneration when injected into rat brains. In contrast, HEWL fibrils were little or non-toxic. The impact of HEWL oligomers on neurons in culture is in line with recent studies showing the *in vitro* toxicity of oligomers from other proteins to different cell types (e.g. Bucciantini *et al.* 2002; Kayed *et al.* 2003; Sirangelo *et al.* 2004; Malisauskas *et al.* 2005). Those recent studies have indicated that soluble oligomers are more cytotoxic than mature amyloid fibrils from the corresponding proteins. Extending this concept, our present results demonstrate that oligomers from a non-disease related protein can also be toxic *in vivo,* while injection of fibrils caused much less neurodegeneration in rat brains.

Remarkably, we found that HEWL oligomers instigate tau hyperphosphorylation in cortical neurons in culture. Tau hyperphosphorylation is a major facet of AD pathology, and it has been recently shown to be induced by soluble Aβ oligomers (De Felice *et al.* 2007b). Under physiological conditions, tau stabilizes neuronal microtubules. However, in AD and in other tauopathies, tau undergoes aberrant hyperphosphorylation, which appears to be related to microtubule destabilization and neurodegeneration (Goedert 1998; Ávila *et al.* 2004). Tau has been implicated as a major downstream target of Aβ-induced neurodegeneration and tau-depleted mouse hippocampal neurons are resistant to Aβ (Rapoport *et al.* 2002). *In vivo*, a link between the buildup of Aβ oligomers and tau hyperphosphorylation was proposed in a recent study employing triple transgenic mice that accumulate elevated levels of soluble Aβ oligomers (Oddo *et al.* 2006). Furthermore, tau hyperphosphorylation has also been observed in animal models of Parkinson's disease (Frasier *et al.* 2005) and in bovine spongiform encephalopathy (Bautista *et al.* 2006), pathological conditions in which oligomers from α-synuclein and the prion protein, respectively, appears to play an important roles. The present results show that HEWL oligomers instigate tau hyperphosphorylation at specific epitopes in cortical neuronal cultures, similar to what has been described for Aβ oligomers (De Felice *et al.* 2007b). This suggests that Aβ and HEWL oligomers share a common structural determinant that triggers neuronal tau hyperphosphorylation. We note, however, that HEWL oligomers prepared using our protocol were not recognized by the A11 antibody (Kayed *et al.* 2003) that has been reported to react with Aβ oligomers as well as with oligomers from various proteins. This suggests that the nature of the possible structural determinants shared by HEWL and Aβ oligomers should be further investigated.

Although the underlying mechanisms are still not fully understood, several hypothesis have been proposed to explain the toxicity of protein oligomers, including disruption of membrane integrity and formation of ion channels

(e.g. Arispe *et al.* 1994; Kayed *et al.* 2004; Demuro *et al.* 2005), oxidative stress (Moreira *et al.* 2005; De Felice *et al.* 2007a; reviewed in Mattson 2004), deregulation of cell homeostasis by accumulation of intracellular amyloid (reviewed in Gouras *et al.* 2005), and interaction of extracellular amyloid with protein receptors (e.g. De Felice *et al.* 2007a; reviewed in Klein *et al.* 2007).

An interesting observation of the present study was that injection of HEWL oligomers in the S1 cortical region of rats caused neurodegeneration in memory-related brain regions, including the hippocampus and amygdala, as early as 8 days after injection. A previous study showed that injection of Aβ fibrils into the somatosensory cortex and hippocampus of P301L tau transgenic mice caused tau hyperphosphorylation in the amygdala (Gotz *et al.* 2001). Those authors concluded that tau phosphorylation in amygdala neuronal cell bodies was caused by damage to the axons of those neurons projecting to the injected hippocampus. Along a similar line, a recent study showed that cholinergic neurons exposed to Aβ oligomers exclusively in distal axons undergo axonal degeneration and subsequent apoptosis, demonstrating that exposure of axon terminals to amyloid oligomers is sufficient to trigger neuronal death (Song *et al.* 2006). In our study, we have observed neuronal degeneration in the S2 region, which is strongly connected with the injection site, as well as in areas that do not heavily project to the injection site (e.g. hippocampus and amygdala). Thus, an alternative possibility suggested by our results is that the soluble HEWL oligomers undergo diffusion in the brain and cause neurodegeneration at sites relatively distal from the site of injection. In the context of AD, this could suggest that Aβ oligomers generated at specific sites might diffuse to and affect neuronal function in other brain areas as well. In this regard, it is important to note that such diffusible Aβ oligomers (also known as ADDLs) are now considered to be the main neurotoxins responsible for neuronal dysfunction in AD (Klein 2006).

In conclusion, the present results support the notion that the neurotoxicity of protein oligomers may not be necessarily related to the specific amino acid sequence of the constituent proteins. Rather, the generic toxicities of oligomers appear to be caused by shared conformation-dependent mechanisms (Bucciantini *et al.* 2002; Kayed *et al.* 2003). In particular, neurodegeneration and tau hyperphosphorylation in AD have been proposed to be triggered by neuronal exposure to soluble Aβ oligomers (reviewed in Klein 2006). Our current findings suggest that oligomers from a non-disease related protein can mimic the neuronal impact of Aβ oligomers, underlining the emerging roles of soluble oligomers in amyloid diseases. Improved understanding of the conformational basis of neuronal impact of soluble protein oligomers may provide important insight to guide the development of novel, effective anti-oligomer therapeutics for AD and other amyloid diseases.

Acknowledgements

We are grateful to Professor Ferenc Gallyas (University of Pecs, Hungary) for expert advice and fruitful discussions regarding experimental approaches for detection of neurodegeneration and to Professor Roberto Lent (Federal University of Rio de Janeiro, Brazil) for support and partial use of his lab facilities. This work was supported by grants from Howard Hughes Medical Institute (STF), Conselho Nacional de Desenvolvimento Científico e Tecnológico (CNPq), Fundação de Amparo à Pesquisa do Estado do Rio de Janeiro and Pronex/FAPERJ (to STF, FGF, and JCH). MNNV is recipient of a pre-doctoral fellowship from Coordenacao de Aperfeicoamento do Pessoal de Ensino Superior, and LFG was recipient of an undergraduate fellowship from CNPq. STF is a Howard Hughes Medical Institute International Scholar, and FGF is a Fellow of the Human Frontier Science Program.

References

Abramoff M. D., Magelhaes P. J. and Ram S. J. (2004) Image processing with imageJ. *Biophotonics Int.* **11**, 36–42.

Arispe N., Pollard H. B. and Rojas E. (1994) The ability of amyloid beta-protein [A beta P (1-40)] to form Ca2+ channels provides a mechanism for neuronal death in Alzheimer's disease. *Ann. NY Acad. Sci.* **747**, 256–266.

Avila J. (2006) Tau phosphorylation and aggregation in Alzheimer's disease pathology. *FEBS Lett.* **580**, 2922–2927.

Ávila J., Lucas J. J., Perez M. and Hernandez F. (2004) Role of tau protein in both physiological and pathological conditions. *Physiol. Rev.* **84**, 361–384.

Bautista M. J., Gutierrez J., Salguero F. J., Fernandez de Marco M. M., Romero-Trevejo J. L. and Gomez-Villamandos J. C. (2006) BSE infection in bovine PrP transgenic mice leads to hyperphosphorylation of tau-protein. *Vet. Microbiol.* **115**, 293–301.

Booth D. R., Sunde M., Bellotti V. *et al.* (1997) Instability, unfolding and aggregation of human lysozyme variants underlying amyloid fibrillogenesis. *Nature* **385**, 787–793.

Bouchard M., Zurdo J., Nettleton E. J., Dobson C. M. and Robinson C. V. (2000) Formation of insulin amyloid fibrils followed by FTIR simultaneously with CD and electron microscopy. *Protein Sci.* **9**, 1960–1967.

Bucciantini M., Giannoni E., Chiti F., Baroni F., Formigli L., Zurdo J., Taddei N., Ramponi G., Dobson C. M. and Stefani M. (2002) Inherent toxicity of aggregates implies a common mechanism for protein misfolding diseases. *Nature* **416**, 507–511.

Canet D., Last A. M., Tito P., Sunde M., Spencer A., Archer D. B., Redfield C., Robinson C. V. and Dobson C. M. (2002) Local cooperativity in the unfolding of an amyloidogenic variant of human lysozyme. *Nat. Struct. Biol.* **9**, 308–315.

De Felice F. G., Vieira M. N., Meirelles M. N., Morozova-Roche L. A., Dobson C. M. and Ferreira S. T. (2004a) Formation of amyloid aggregates from human lysozyme and its disease-associated variants using hydrostatic pressure. *FASEB J.* **18**, 1099–1101.

De Felice F. G., Vieira M. N., Saraiva L. M., Figueroa-Villar J. D., Garcia-Abreu J., Liu R., Chang L., Klein W. L. and Ferreira S. T. (2004b) Targeting the neurotoxic species in Alzheimer's disease: inhibitors of Abeta oligomerization. *FASEB J.* **18**, 1366–1372.

De Felice F. G., Velasco P. T., Lambert M. P., Viola K., Fernandez S. J., Ferreira S. T. and Klein W. L. (2007a) Abeta oligomers induce neuronal oxidative stress through an N-methyl-D-aspartate receptor-dependent mechanism that is blocked by the Alzheimer drug memantine. *J. Biol. Chem.* **282**, 11590–11601.

De Felice F. G., Wu D., Lambert M. P. *et al.*(2007b) Alzheimer's disease-type neuronal tau hyperphosphorylation induced by Abeta oligomers. *Neurobiol. Aging* Epub ahead of print. DOI:10.1016/j.neurobiolaging.2007.02.029.

Demuro A., Mina E., Kayed R., Milton S. C., Parker I. and Glabe C. G. (2005) Calcium dysregulation and membrane disruption as a ubiquitous neurotoxic mechanism of soluble amyloid oligomers. *J. Biol. Chem.* **280**, 17294–17300.

Dobson C. M. (1999) Protein misfolding, evolution and disease. *Trends Biochem. Sci.* **24**, 329–332.

Dobson C. M., Evans P. A. and Radford S. E. (1994) Understanding how proteins fold: the lysozyme story so far. *Trends Biochem. Sci.* **19**, 31–37.

Fandrich M., Fletcher M. A. and Dobson C. M. (2001) Amyloid fibrils from muscle myoglobin. *Nature* **410**, 165–166.

Ferreira S. T., De Felice F. G. and Chapeaurouge A. (2006) Metastable, partially folded states in the productive folding and in the misfolding and amyloid aggregation of proteins. *Cell Biochem. Biophys.* **44**, 539–548.

Ferreira S. T., Vieira M. N. and De Felice F. G.(2007) Soluble protein oligomers as emerging toxins in Alzheimer's and other amyloid diseases. *IUBMB Life* **59**, 332–345.

Frasier M., Walzer M., McCarthy L., Magnuson D., Lee J. M., Haas C., Kahle P. and Wolozin B. (2005) Tau phosphorylation increases in symptomatic mice overexpressing A30P alpha-synuclein. *Exp. Neurol.* **192**, 274–287.

Goedert M. (1998) Filamentous nerve cell inclusions in neurodegenerative diseases: tauopathies and alpha-synucleinopathies. *Philos. Trans. R. Soc. Lond. B Biol. Sci.* **354**, 1101–1118.

Gotz J., Chen F., van Dorpe J. and Nitsch R. M. (2001) Formation of neurofibrillary tangles in P301 L tau transgenic mice induced by Abeta 42 fibrils. *Science* **293**, 1491–1495.

Gouras G. K., Almeida C. G. and Takahashi R. H. (2005) Intraneuronal Abeta accumulation and origin of plaques in Alzheimer's disease. *Neurobiol. Aging* **26**, 1235–1244.

Guijarro J. I., Sunde M., Jones J. A., Campbell I. D. and Dobson C. M. (1998) Amyloid fibril formation by an SH3 domain. *Proc. Natl Acad. Sci. USA* **95**, 4224–4228.

Haass C. and Selkoe D. J. (2007) Soluble protein oligomers in neurodegeneration: lessons from the Alzheimer's amyloid beta-peptide. *Nat. Rev. Mol. Cell Biol.* **8**, 101–112.

Hampel H., Goernitz A. and Buerger K. (2003) Advances in the development of biomarkers for Alzheimer's disease: from CSF total tau and Abeta(1-42) proteins to phosphorylated tau protein. *Brain Res. Bull.* **61**, 243–253.

Hoshi M., Sato M., Matsumoto S., Noguchi A., Yasutake K., Yoshida N. and Sato K. (2003) Spherical aggregates of beta-amyloid (amylospheroid) show high neurotoxicity and activate tau protein kinase I/glycogen synthase kinase-3beta. *Proc. Natl Acad. Sci. USA* **27**, 6370–6375.

Kayed R., Head E., Thompson J. L., McIntire T. M., Milton S. C., Cotman C. W. and Glabe C. G. (2003) Common structure of soluble amyloid oligomers implies common mechanism of pathogenesis. *Science* **300**, 486–489.

Kayed R., Sokolov Y., Edmonds B., McIntire T. M., Milton S. C., Hall J. E. and Glabe C. G. (2004) Permeabilization of lipid bilayers is a common conformation-dependent activity of soluble amyloid oligomers in protein misfolding diseases. *J. Biol. Chem.* **279**, 46363–46366.

Kelly J. W. (2000) Mechanisms of amyloidogenesis. *Nat. Struct. Biol.* **7**, 824–826.

Klein W. L. (2006) Synaptic targeting by Aβ oligomers (ADDLs) as a basis for memory loss in early Alzheimer's disease. *Alzheimer's Dement.* **2**, 43–55.

Klein W. L., Stine Jr W. B. and Teplow D. B. (2004) Small assemblies of unmodified amyloid beta-protein are the proximate neurotoxin in Alzheimer's disease. *Neurobiol. Aging* **25**, 569–580.

Klein W. L., Lacor P. N., De Felice F. G. and Ferreira S. T. (2007) Molecules that disrupt memory circuits in Alzheimer's disease: the attack on synapses by Aβ oligomers (ADDLs), in *Memories: Molecules and Circuits* (Bontempi B, Silva A. and Christen Y., eds.), pp. 155–179. Springer, Paris.

Krebs M. R., Wilkins D. K., Chung E. W., Pitkeathly M. C., Chamberlain A. K., Zurdo J., Robinson C. V. and Dobson C. M. (2000) Formation and seeding of amyloid fibrils from wild-type hen lysozyme and a peptide fragment from the beta-domain. *J. Mol. Biol.* **300**, 541–549.

Lambert M. P., Barlow A. K., Chromy B. A. *et al.* (1998) Diffusible, nonfibrillar ligands derived from Abeta1-42 are potent central nervous system neurotoxins. *Proc. Natl Acad. Sci. USA* **95**, 6448–6453.

Lashuel H. A., Hartley D. M., Petre B. M., Wall J. S., Simon M. N., Walz T. and Lansbury Jr P. T. (2003) Mixtures of wild-type and a pathogenic (E22G) form of Abeta40 in vitro accumulate protofibrils, including amyloid pores. *J. Mol. Biol.* **332**, 795–808.

Lindgren M., Sorgjerd K. and Hammarstrom P. (2005) Detection and characterization of aggregates, prefibrillar amyloidogenic oligomers, and protofibrils using fluorescence spectroscopy. *Biophys. J.* **88**, 4200–4212.

Maccioni R. B, Lavados M., Guillon M., Mujica C., Bosch R., Farias G. and Fuentes P. (2006) Anomalously phosphorylated tau and Abeta fragments in the CSF correlates with cognitive impairment in MCI subjects. *Neurobiol. Aging* **27**, 237–244.

Malisauskas M., Ostman J., Darinskas A., Zamotin V., Liutkevicius E., Lundgren E. and Morozova-Roche L. A. (2005) Does the cytotoxic effect of transient amyloid oligomers from common equine lysozyme in vitro imply innate amyloid toxicity? *J. Biol. Chem.* **280**, 6269–6275.

Mattson M. P. (2004) Pathways towards and away from Alzheimer's disease. *Nature* **430**, 631–639.

Moreira P. I., Honda K., Liu Q. *et al.* (2005) Oxidative stress: the old enemy in Alzheimer's disease pathophysiology. *Curr. Alzheimer Res.* **2**, 403–408.

Morozova-Roche L. A., Zurdo J., Spencer A., Noppe W., Receveur V., Archer D. B., Joniau M. and Dobson C. M. (2000) Amyloid fibril formation and seeding by wild-type human lysozyme and its disease-related mutational variants. *J. Struct. Biol.* **130**, 339–351.

Nandi P. K. and Nicole J. C. (2004) Nucleic acid and prion protein interaction produces spherical amyloids which can function in vivo as coats of spongiform encephalopathy agent. *J. Mol. Biol.* **344**, 827–837.

Oddo S., Caccamo A., Tran L., Lambert M. P., Glabe C. G., Klein W. L. and Laferla F. M. (2006) Temporal profile of amyloid-beta (Abeta) oligomerization in an in vivo model of Alzheimer disease. A link between Abeta and tau pathology. *J. Biol. Chem.* **281**, 1599–1604.

Pepys M. B., Hawkins P. N., Booth D. R. *et al.* (1993) Human lysozyme gene mutations cause hereditary systemic amyloidosis. *Nature* **362**, 553–557.

Pertinhez T. A., Bouchard M., Tomlinson E. J. *et al.* (2001) Amyloid fibril formation by a helical cytochrome. *FEBS Lett.* **495**, 184–186.

Rapoport M., Dawson H. N., Binder L. I., Vitek M. P. and Ferreira A. (2002) Tau is essential to beta-amyloid-induced neurotoxicity. *Proc. Natl Acad. Sci. USA* **99**, 6364–6369.

Ray S. S., Nowak R. J., Strokovich K., Brown Jr R. H., Walz T. and Lansbury Jr P. T. (2004) An intersubunit disulfide bond prevents in vitro aggregation of a superoxide dismutase-1 mutant linked to familial amytrophic lateral sclerosis. *Biochemistry* **43**, 4899–4905.

Schmued L. C., Stowers C. C., Scallet A. C. and Xu L. (2005) Fluoro-Jade C results in ultra high resolution and contrast labeling of degenerating neurons. *Brain Res.* **1035**, 24–31.

Sirangelo I., Malmo C., Iannuzzi C., Mezzogiorno A., Bianco M. R., Papa M. and Irace G. (2004) Fibrillogenesis and cytotoxic activity of the amyloid-forming apomyoglobin mutant W7FW14F. *J. Biol. Chem.* **279**, 13183–13189.

Song M. S., Saavedra L. and de Chaves E. I. (2006) Apoptosis is secondary to non-apoptotic axonal degeneration in neurons exposed to Abeta in distal axons. *Neurobiol. Aging* **27**, 1224–1238.

Sreerama N. and Woody R. W. (2000) Estimation of protein secondary structure from circular dichroism spectra: comparison of CONTIN, SELCON and CDSSTR methods with an expanded reference set. *Anal. Biochem.* **287**, 252–260.

Stefani M. and Dobson C. M. (2003) Protein aggregation and aggregate toxicity: new insights into protein folding, misfolding diseases and biological evolution. *J. Mol. Med.* **81**, 678–699.

Valleix S., Drunat S., Philit J. B., Adoue D., Piette J. C., Droz D., MacGregor B., Canet D., Delpech M. and Grateau G. (2002) Hereditary renal amyloidosis caused by a new variant lysozyme W64R in a French family. *Kidney Int.* **61**, 907–912.

Vieira M. N., Figueroa-Villar J. D., Meirelles M. N., Ferreira S. T. and De Felice F. G. (2006) Small molecule inhibitors of lysozyme amyloid aggregation. *Cell Biochem. Biophys.* **44**, 549–553.

Walsh D. M. and Selkoe D. J. (2004) Deciphering the molecular basis of memory failure in Alzheimer's disease. *Neuron* **44**, 181–193.

Walsh D. M., Klyubin I., Fadeeva J. V., Cullen W. K., Anwyl R., Wolfe M. S., Rowan M. J. and Selkoe D. J. (2002) Naturally secreted oligomers of amyloid beta protein potently inhibit hippocampal long-term potentiation in vivo. *Nature* **416**, 535–539.

Wang H. W., Pasternak J. F., Kuo H. *et al.* (2002) Soluble oligomers of beta amyloid, 1-42, inhibit long-term potentiation but not long-term depression in rat dentate gyrus. *Brain Res.* **924**, 133–140.

Yazaki M., Farrell S. A. and Benson M. D. (2003) A novel lysozyme mutation Phe57Ile associated with hereditary renal amyloidosis. *Kidney Int.* **63**, 1652–1657.

Zheng-Fischhofer Q., Biernat J., Mandelkow E. M., Illenberger S., Godemann R. and Mandelkow E. (1998) Sequential phosphorylation of Tau by glycogen synthase kinase-3beta and protein kinase A at Thr212 and Ser214 generates the Alzheimer-specific epitope of antibody AT100 and requires a paired-helical-filament-like conformation. *Eur. J. Biochem.* **252**, 542–552.